A 21 CM LINE STUDY OF THE TAURUS MOLECULAR COMPLEX

by

CALVIN GLENN KLATT

A THESIS SUBMITTED IN PARTIAL FULFILMENT OF

THE REQUIREMENTS FOR THE DEGREE OF

MASTER OF APPLIED SCIENCE

in

THE FACULTY OF GRADUATE STUDIES

PHYSICS

We accept this thesis as conforming

to the required standard

THE UNIVERSITY OF BRITISH COLUMBIA

August 1986

In presenting this thesis in partial fulfilment of the requirements for an advanced degree at the The University of British Columbia, I agree that the Library shall make it freely available for reference and study. I further agree that permission for extensive copying of this thesis for scholarly purposes may be granted by the Head of my Department or by his or her representatives. It is understood that copying or publication of this thesis for financial gain shall not be allowed without my written permission.

PHYSICS

The University of British Columbia
2075 Wesbrook Place
Vancouver, Canada
V6T 1W5

Date: <u>August 1986</u>

Abstract

The large scale distribution of 21 cm self absorption in the Taurus Molecular Complex has been determined from observations made by us at Arecibo Observatory in October 1985. Results have been compared with ^{13}CO previously observed by Kleiner and Dickman at FCRAO.

The principal conclusions drawn from a two-dimensional auto and cross-correlation analysis are:

(1) The cold atomic hydrogen in the Taurus Complex has an extremely well defined condensation scale length of 14 pc, as was found for CO.

(2) The 21 cm and CO column densities are essentially uncorrelated. Previous thinking would have predicted a high degree of correlation if the HI and CO were well mixed, or a high degree of anticorrelation if the atomic hydrogen was distributed in shells around the molecular gas.

Table of Contents

List of Figures

Acknowledgements

I would like to thank my supervisor, W.L.H. Shuter, for his guidance and assistance throughout this project and for his financial support.

I would also like to thank Marcus Aurelius for keeping a diary, my Mother for her help, and Dr. S. David for the education she gave me.

Finally, thanks to the many fine people who have been supportive of me over the last two years, and whose friendship I value very highly.

Let us begin from Zeus, whom we mortals never leave unnamed. Full of Zeus are all streets, all meetingplaces of men, full are seas and harbours; every way we stand in need of Zeus. We are even his offspring; he, in his kindness to man, points out things of good omen, rouses the people to labour, calling to their minds the needs of daily life, tells them when the soil is best for the labour of the ox and for the pick, and when the seasons are propitious for planting trees and all manner of seeds. For he it was who fixed the signs in the heaven, and set apart the constellations, and he who, looking to the year, determined which of the stars were best fitted to mark the seasons for men, so that things might grow unfailingly. For this cause men ever worship him, first and last. Hail, O Father, Great Wonder, great blessing to mankind, hail to thyself and to thy elder line. Hail, ye Muses, most gracious all; and for me who presume to tell of the stars, so far as I rightly may, guide ye all my song.

ARATUS, Phaenomena

I. <u>INTRODUCTION</u>

Little more than a decade ago giant molecular clouds (GMC's) were unknown. With the discovery of these bodies came the realization of the extent of molecular gas in our galaxy, and of its role in star formation. Previously, it was believed that virtually all of the hydrogen gas in the interstellar medium was in atomic form, or ionized due to high radiation flux. Young stars ('young' refers to stars whose great masses imply very short lifetimes, putting an upper limit on their age) were thought to arise from clouds of atomic hydrogen, but now it is known that these GMC's are the true birthplaces.

Giant molecular clouds are the largest single entities in the galaxy, with masses ranging from 10^5 to 10^6 Solar Masses ($M_\odot$). An understanding of these clouds leads to an understanding of how different sizes of stars are formed, how frequently they form, and what regulates the rate and type of star formation. They also play a substantial role in the overall galactic structure, especially with respect to spiral density waves in which they seem to cluster and with which they are evidently associated.

Molecular clouds went unstudied (unnoticed) for such a long time because their particular composition made them appear only as dark regions in the sky. As their name implies, their principal component is molecular hydrogen. In much lesser quantities are found neutral hydrogen atoms (HI) from which the molecular clouds likely condensed, and

Helium. Very important, but small amounts of other
constituents exist as well: many complex molecules have been
found in the cold dense environs of GMC's. A final
ingredient, of great importance, is the grains of dust which
are responsible for the dark appearance of the clouds.

These dust grains, believed to be composed of carbon
and silicates, constitute about 1% of the clouds by mass.
The dust grain size and composition makes them very
effective absorbers of visual and untraviolet radiation,
which they re-emit in the infrared. Fortunately, however,
the grains do not hinder infrared or radio frequency
radiation.

It was only with the extension of astronomical
observations into the infrared and mm-wavelength regions
(with technological advancement) that giant molecular clouds
were observable as sources rather than as dark areas.
Infrared observations today reveal previously unobserved
stars imbedded in the dark, dusty clouds. These stars are
believed to be newly metamorphosed from cold gas, and their
observation constitutes the closest thing astronomers have
to watching the process of star formation. All nearby
molecular clouds (within 2 kpc) seem to show evidence of
recent star formation, illustrating their ongoing role in
the galactic drama.

This study aims to increase our understanding of the
relationship between the molecular and atomic hydrogen
within an individual cloud. A previous observational

program, conducted by Stephen Kleiner and Robert Dickman of the University of Massachusetts (see Kleiner, 1985, or Kleiner, Dickman, 1985, papers I,II,III) involved mapping (indirectly) the H_2 column density and velocity structure of the Taurus molecular complex. The present work involves observing the atomic hydrogen content in this cloud on an identical grid to that of the molecular work.

Simple observation of the two maps will provide some insight into the mixing of these two cloud components. The principal aim, however, is the use of statistical methods (auto and cross-correlation) to look for average trends in the velocity and column density structure. These statistical methods measure the mean degree of correlation between two data sets, or of one data set with itself, as a function of vector offset. The two dimensional autocorrelation function was employed in the H_2 study mentioned, and the present study uses the same measure on atomic hydrogen data. The use of identical grids for observations is necessary for comparison of maps and autocorrelation surfaces, and also allows us to cross-correlate atomic and molecular hydrogen data.

The molecular hydrogen observations prior to this work proved to be of some interest. The autocorrelation of velocity data did not demonstrate any statistically meaningful peaks, but that of the column density data did. A secondary peak (the primary peak is the large self-correlation peak at zero offset) on the column density

autocorrelation surface was observed at a projected distance
of approximately 14 pc. This secondary peak can be regarded
as a mean scale size of clumpiness in the molecular hydrogen
content of the Taurus complex.

Our observations of the neutral hydrogen proved even
more interesting. Both the velocity and column density
autocorrelations produced secondary peaks at scale sizes
only slightly greater than that of the H_2 column density, at
approximately the same orientation. This is even more
interesting in light of the difference between the two maps:
the structure of the two elements within the cloud appear
remarkably different. The neutral hydrogen displays neither
of the two expected structures: no HI shell around the H_2
appears, nor does the HI have the same structure as the H_2!
This result is borne out by the cross-correlation of the two
column density data sets, with neither strong correlation
nor anticorrelation evident. Perhaps a greater surprise was
to be found in the velocity maps of the region. The
molecular hydrogen was observed to have a large gradient
across the field, indicative of rotation. The atomic
hydrogen was found to rotate as well, but in the opposite
direction! The axes of rotation appear to be one and the
same, suggesting a single physical explanation.

The common scale length in the two data sets which have
significantly different appearance suggests that a process
common to the two components has been unveiled by the
analysis. It was suggested of the scale length discovered in

the H_2 column density data that it was a remnant of the initial formation of the molecular cloud from neutral hydrogen. This suggestion, referred to as a "fossil scale length" by the authors of the H_2 study, appears to be borne out by the appearance of similar scale lengths in our observations.

II. PHYSICAL CONSIDERATIONS

The recent extension of radio astronomy into the millimeter wavelength region has provided us with the ability to observe the structure of the cold gas itself. At the temperatures characteristic of these clouds, H_2 gas is not directly observable, but an indirect method of observation has been developed. One of the trace molecules in the clouds' composition is CO, which is observable at redio wavelengths and seems to be coextensive with the H_2 gas. These CO molecules are excited (in rotational energy) by collisions with the H_2 molecules (much more common than CO or any other constituent) and emit mm-wavelength spectral line radiation.

The ratio of CO to H_2 column densities is believed to be approximately uniform in dark clouds, and hence measuring CO column densities allows one to infer H_2 column densities. The CO is believed to exist in a thermal distribution of energy levels, with the transition between J=0 and J=1 strong and relatively easy to observe. Two families of CO exist and are observable, ^{13}CO and ^{12}CO, with the ^{12}CO line optically thicker and hence more likely to saturate.

This study attempts to increase our understanding of the structure and formation of molecular clouds through observing their neutral hydrogen content. The hyperfine spin-flip transition of neutral hydrogen at 1420.4 MHz or 21 cm was the first interstellar radio frequency spectral line observed and remains one of the most important. This line
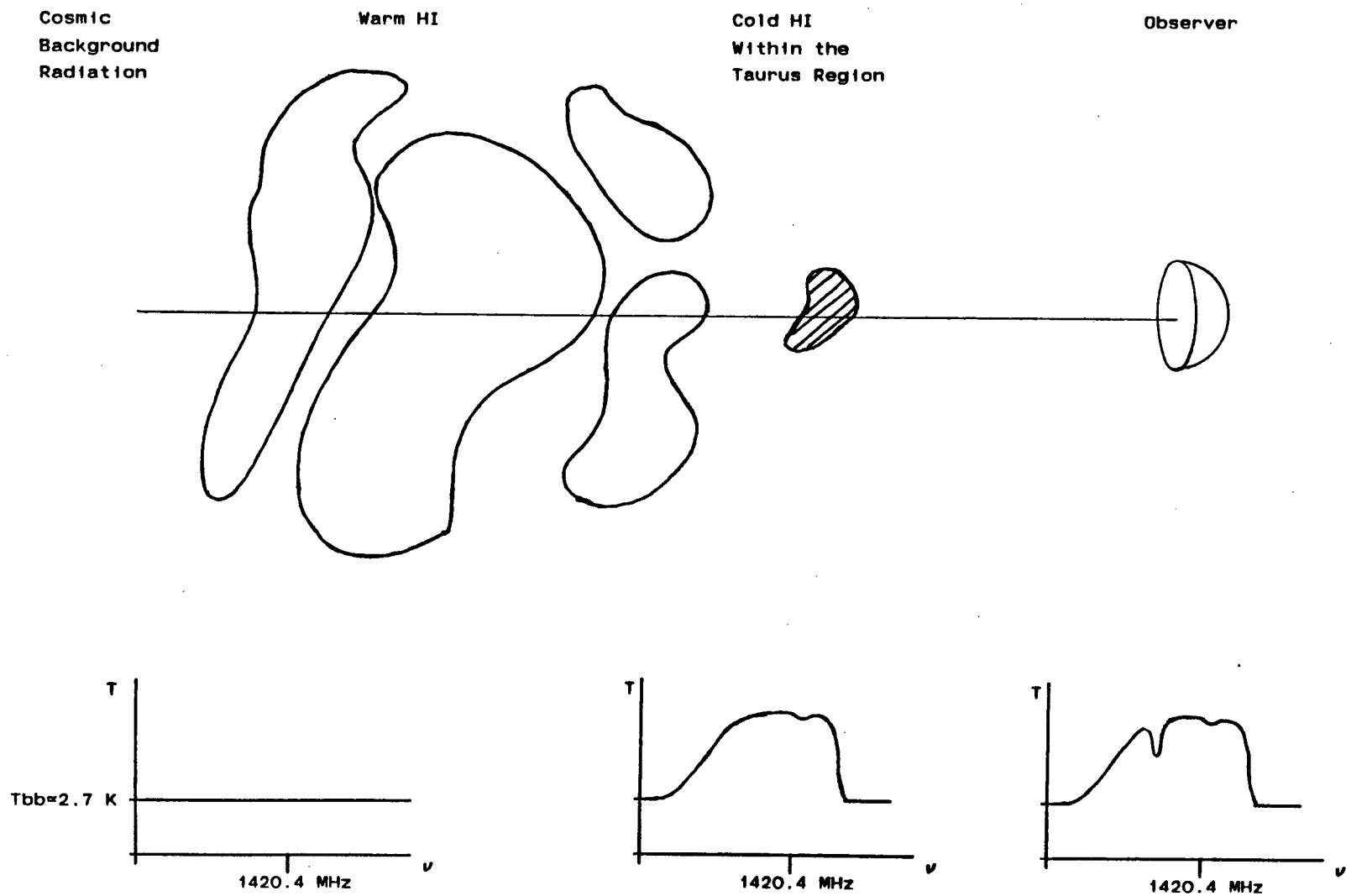
can be observed in every direction in the sky, emitted by the warm HI gas which exists throughout the galaxy. Cold HI, as exists in and/or around molecular clouds, is generally seen in absorption of radiation from warmer (hence brighter) background sources. It is the 21 cm spectral line self-absorption which we use in this observational program to estimate column densities of neutral hydrogen across the projected face of the Taurus molecular complex.

Figure 1 on the following page illustrates the situation as we interpret it. A continuum radiation of 2.7 K, likely the remnant from the big bang, is the first element. Added to this background is the 21 cm emission from warm HI sources, which will have varying amounts of line structure. This radiation then impinges on the cold cloud, where the cold neutral hydrogen contents absorb energy in a narrow spectral line. The background spectral line is broadened by differential galactic rotation along the line of sight, turbulent motion, and thermal effects. The absorption feature results from a compact region of cold gas, and is consequently quite narrow.

If the background sources are generally free from structure and little foreground material exists between the cold cloud and the observer, the absorption feature will be easily identifiable, as shown.

Our present knowledge of molecular clouds is substantial, but a profusion of information has not provided us with a simple picture of the principal mechanisms

Figure 1: 21cm Self Absorption

Cosmic
Background
Radiation

Warm HI

Cold HI
Within the
Taurus Region

Observer

Tbb≈2.7 K

1420.4 MHz

1420.4 MHz

1420.4 MHz

involved in their evolution. These cloud complexes vary greatly in size and in complexity of structure, some small and roughly spherical, others extended and knotty. It is clear that the individual histories of the clouds, which have determined their structure, differ substantially. A goal of this research is to look at the underlying average clumpiness of one large complex with a view towards obtaining a common metre-stick by which all such clouds can be measured. It is to be hoped that our metre-stick, the column density and velocity autocorrelation functions, provides us with measurements which can be understood in terms of the physical environment common to the clouds.

The giant molecular clouds experience a large range of external and internal processes that govern their structure. External perturbations involve such things as galactic tidal forces, cosmic ray heating, density wave interactions, supernova blast waves, stellar winds, cloud-cloud interactions, and (gravitational) interactions with other objects. Internal processes also play a major role, with gravitational forces collapsing the clouds, radiation from embedded stars expanding nearby gas and magnetic fields restricting collapse. These many processes combine in various ways to produce the many cloud shapes observed, but their relative importances in the overall picture is as of yet undetermined.

It is well understood at what mean temperature, density, and molecular weight self-gravitational

instabilities arise in a medium. This threshold is governed by the Jeans criterion, and can be expressed, for our purposes, as a Jeans length. Many observed clouds are clearly unstable by simple application of this criterion (ignoring factors other than self-gravitation), so many, in fact, as to conflict with observed star formation rates. Incorporation of other processes into the criterion lowers the expected star formation rate.

Further complications arise from spectral line observations of cold clouds which display line widths which are unattributable to thermal motion. Turbulent gas motions are now accepted to be a common feature of these cold clouds, and such motions are inherently unpredictable.

It is also unclear how the various components of these clouds are mixed. It has been suggested that neutral hydrogen forms a rough halo around the molecular hydrogen; expected if the neutral hydrogen temperature were higher than that of the H_2. Alternatively, if the HI were produced out of the H_2 by cosmic ray heating, for example, the two species should have the same distribution within the cloud.

One clear result of this observing program will be a fair comparison of the two distributions. Inspection of the CO and HI column densities and velocity maps alone will be informative. The statistical results will provide measures of mean scale sizes of the condensations within each of the two hydrogen components.

The evolution of giant molecular clouds is clearly not a smooth process. Internal forces disrupt star formation, while successful star formation disturbs large areas, possibly triggering further collapse, possibly dispersing regions which might have otherwise collapsed. The violent interplay of giant molecular clouds and their galactic environment also plays a large role in their structure, their stability, and their rates of star formation.

III. OBSERVATIONS AND DATA REDUCTION

A. OBSERVATIONS

Studied in this work was the Taurus molecular complex, approximately centred at (1950) coordinates a = 4h 30m, δ = +27° (lII = 172, bII = -14). This complex is a large region of irregular patchy dark clouds at a distance of approximately 140 pc (see Elias, 1978), and believed to contain about 10^6 M$_\odot$ of material, with most of the hydrogen in molecular form.

For the study of this cloud's molecular hydrogen portion, Kleiner and Dickman (1985) made indirect determinations of the molecular hydrogen column density and centroid velocity. This was done by observing the J=1 to 0 rotational transition of ^{13}CO and employing an expected fixed ratio of ^{13}CO to H$_2$ in clouds of this type (see Chapter II).

The present study focusses on the structure of the neutral hydrogen (HI) in this cloud, and employs the hyperfine (spin-flip) transition at 1420.4 MHz (λ=21 cm) in self-absorption.

Our choice of the Taurus cloud complex was made for several reasons. The cloud is conveniently located sufficiently displaced from the galactic plane for the HI emission from warm background sources to be relatively free of complicated structure, necessary for absorption studies of extended objects. Also, the relative proximity

(distance≃140 pc) of the Taurus complex is very important in that little foreground material complicates the study, and high spatial resolution is obtained. This complex also seems to be free of the disruptive effects of O stars or embedded HII regions. It was for similar reasons that Kleiner and Dickman studied this cloud, and the availability of their data constitutes the final reason for our choice of the Taurus complex.

The complex seems to lie at the tip of a dusty region extending towards the sun at an angle of about 60° with respect to the plane of the sky. If the gas can be assumed to generally lie along this axis, then a correction for simple geometric foreshortening of $(1/\cos\theta)=2$ should be used. This correction is applied to all scale lengths obtained in the analysis.

The CO observations of this cloud were made at the Five College Radio Astronomy Observatory (FCRAO) operated by the University of Massachusetts, which at the 2.7 mm wavelength of operation had a beamwidth of only 48 arcsec. It was necessary that our observations be made at the exact same positions as was the CO study. To correctly sample at the 1/4° (15 arcmin) intervals used in the FCRAO work, we required a beamwidth much smaller than the sampling interval, and low antenna beam sidelobes so as to avoid information smearing between neighboring points.

The Arecibo observatory, located near Arecibo, Puerto

Rico[1], the largest single dish radio telescope in the world, was thus an appropriate choice for our observations. At a wavelength of 21 cm, the beamwidth of this telescope is $\simeq 4$ arcmin, sufficiently less than the 15 arcmin sampling interval, and the sidelobes were at a satisfactory level for our purposes[2]. The limited pointing range of this telescope, resulting from its having a fixed reflector, was not a difficulty for our work, because of our source being conveniently within the "visible" sky for the Arecibo telescope.

In October 1985, 1271 21 cm spectra were observed in a rectangular grid (41 parallel to right ascension by 31 parallel to declination) at $1/4°$ intervals centred at (1950) $a=$4h 30m, $\delta=$+27°. This is an identical grid to that of the CO observations. Power spectra were obtained using a 504 channel autocorrelation spectrometer, with a channel width of 4.88 kHz (1.03 km/sec) and a channel spacing of 2.44 kHz (0.515 km/sec). Integration times varied between 20 and 7 seconds, with large signal to noise ratios in every spectra. The system noise temperature was 60 K.

B. DATA REDUCTION

The 21 cm power spectra were recorded on magnetic tape at the observatory, and brought to the UBC Physics department, Vancouver for reduction on a Sperry microcomputer.

----

[1]The Arecibo Observatory is operated by Cornell University, with funds provided by the NSF.
[2]The 21 cm "Flat feed" was used for these observations.

Calibration was done through repeated observations of coordinates lII = 190°, bII = 0°, and comparison with the intensity of this source in the Weaver and Williams survey[3]. Zenith angle corrections were done only approximately, with estimated errors from this less than 5%. Greater accuracy was not felt to be necessary in this preliminary data reduction because of the much more significant errors involved in the curve fitting procedure used to measure the absorption depth, as discussed below.

The objectives of the data reduction were column density and centroid velocity values at each point in the observed grid. It was thus necessary to estimate the background line temperatures above the background continuum radiation (2.7 K + receiver), throughout the absorption regions on each spectrum. The first step in this procedure was removal of the non-line background through subtraction of a first-order polynomial fit to selected portions of the data.

Absorption features studied were limited to those within the velocity range 0 to 8 km/sec, the expected velocity range of the components of this cloud. This range proved to contain virtually all of the self-absorption features, as we would expect.

The most satisfactory method of estimating background lines in studies of this type is the ON/OFF method, in which spectra are obtained on the absorbing cloud and off it in a
----
[3]The Berkeley low-lattitude survey of neutral hydrogen, 1973.

region sufficiently close that there is little variation of the background radiation. These two spectra are then subtracted, yielding an excellent estimate of the absorption spectra. This method, however, is unavailable for our study because of the considerable extent of our absorbing object.

Absorption studies of extended regions must, of necessity, resort to far less satisfactory techniques of estimation[4]. One of these methods is straight line interpolation, as used by Batrla, *et al*, 1981. This method has an advantage in that it makes few assumptions about the line structure. It unfortunately also severely underestimates the background radiation temperatures, yielding no absorption for a flat top on a spectrum, for instance. Alternatively, Gaussian fits (single or multiple) can be made to the spectra, with the absorbed regions masked. This technique, at first glance appears adequate as well as intellectually satisfying. However, it can easily be shown that 21 cm spectra are much more complex in structure at the observatory than in an introductory astrophysics textbook. Our observed spectra bore little resemblance to a simple Gaussian, or to any simple combination of two or three Gaussians. Two other methods remained; the masked higher-order polynomial and the masked cubic spline[5] interpolators. Both of these two methods make few

---

[4]For a full discussion and comparison of methods, see Levinson and Brown, 1980.
[5]A cubic spline is composed of cubic segments between pairs of data points. A continuity condition between segments is imposed over the first three derivatives. Refer to Schultz, 1973, for a full discussion.

assumptions about the emission structure and are easily implemented.

Our choice was the cubic spline, which is less likely to exhibit unwanted structure in the masked region than the polynomial. As smooth curves were desirable over the masked region, whose true structure was unknown, the cubic spline, with its zero third derivatives over small lengths, performed admirably. Figure 2 on the following page shows the spectrum from the grid centre with a spline fit made (this is a relatively strong absorption).

As with any estimation method, a number of difficulties in implementation arose. For the spline fits, the chief difficulty was in the selection of the region of the spectrum to be masked (the region affected by the absorbing cloud). Different selections provided significantly different curve fits[6]. Masks were selected interactively, and an effort was made to mask the smallest region possible while maintaining a fit over the absorption region which appeared to be (empirically) unaffected by the absorption. Signs of a poor fit are such things as the existence in the interpolated region of local minima or local maxima away from the central emission peak.

----

[6]It should be noted that the spectra were smoothed prior to fitting. Smoothing was performed in the Fourier transform domain by multiplication with a Hamming window function (see Chapter IV) cutting off at 0.205 kHz^{-1}. Too little smoothing adversely affected the attempts to fit over the absorption, while excessive smoothing widened the absorption feature and created great error. A happy medium was, however, easily arrived at.

Figure 2: Spline Fit to the Spectrum at the Map Centre

(a=4h 30m, δ=+27°)
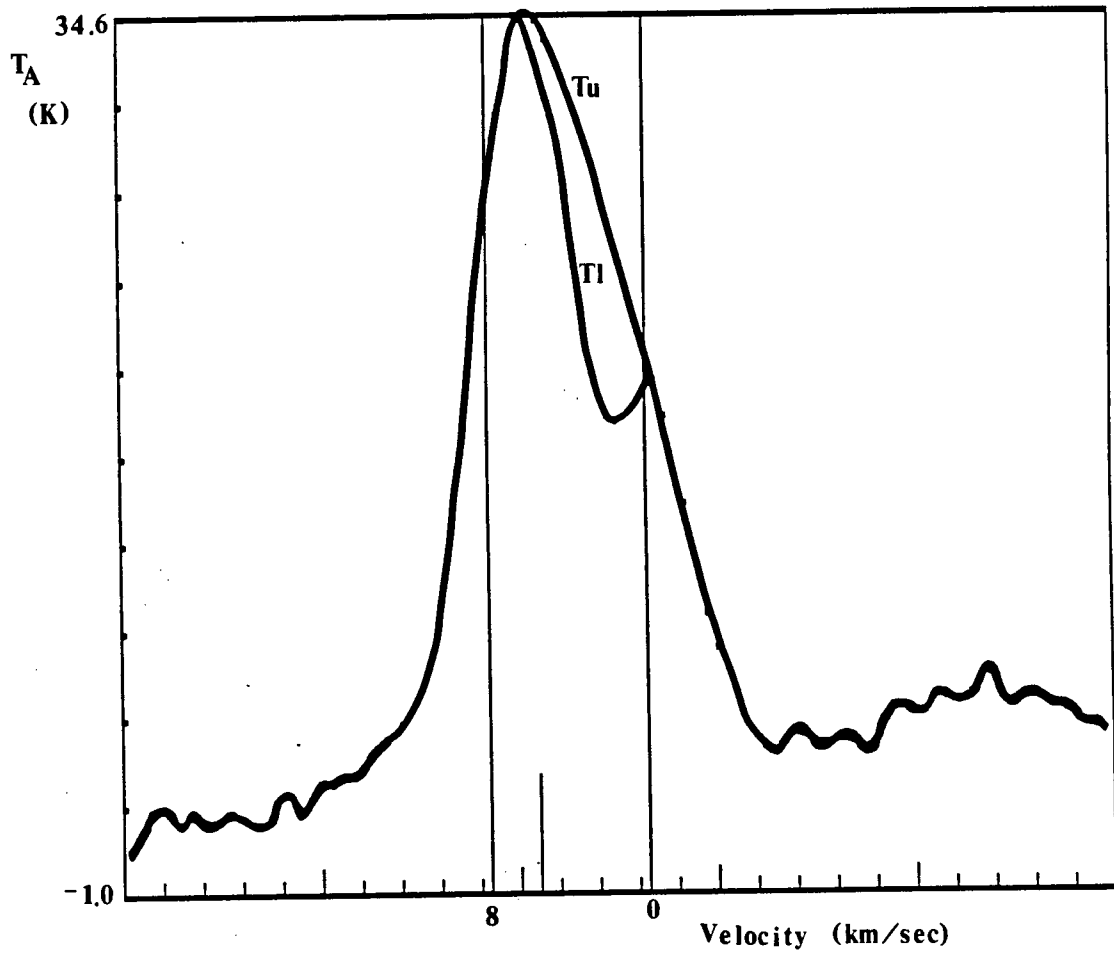
Tbb Subtracted

Masked Region: Approximately 0 to 6 km/sec

It should be noted that the absorption regions were often difficult to determine. Frequently smaller absorptions only showed up as flattened regions on the side of the emission line, with no local minimum to be seen.

Spectra with two regions of absorption were also seen, when overlapping clumps of the Taurus cloud, moving at different velocities, were seen. Column densities for grid points exhibiting this were taken as the sum of that seen in each region, while velocity values were the centroid over the two absorptions. Centroid velocities for spectra having no significant absorption were unattainable, and interpolation techniques proved difficult due to the inhomogeneity of the complex. It was decided that the most advantageous method would be to assign the value of the mean velocity of the entire data set to these unknown velocities. A discussion of the implications of this may be found in Chapter V.

Another difficulty was as a result of hardware errors, in particular spectrometer failures at the observatory. Single channels of the spectrometer unfortunately failed on a few occasions, and repairs were made in the Fourier transform domain (poor spectrometer channels appear as obvious spikes in the transform of the spectra). A number (four) of these spectra had then to be scaled in amplitude and the mean amplitude of its neighbors was used. Only one spectra was irreparable, and the mean column density and centroid velocity of its neighbors was used. The small

number of difficult spectra makes the potentially large errors of no great concern, and it was felt unnecesary to have these observations made again.

Once an acceptable estimate of the background line shape has been made, it remains to calculate column density and centroid velocity. If we define Tu as the (estimated) unabsorbed line temperature at some frequency, Tl as the (observed) absorbed temperature, Tspin as the spin temperature of the absorbing gas, and Tbb as the cosmic background radiation ($\simeq 2.7$ K), then the optical depth at this frequency is given by[7]:

τ = ln((Tu-Tspin+Tbb)/(Tl-Tspin+Tbb))

Column density values are then given by:

CD = 1.823 * 10^{18} * Tspin * $\int \tau$*dV (/cm^2), dV in km/sec

Centroid velocities are calculated, where possible, in the following manner:

V = ($\int$(Tu-Tl)*V*dV) / ($\int$(Tu-Tl)*dV)

In these calculations, the chief assumption was in setting a value to the spin temperature of the cloud. It is clear that Tspin is less than or equal to the lowest temperature value within the absorption region on any given spectrum, since absorption ceases at Tspin=Tl+Tbb.

It does not appear that line saturation has occurred frequently in our observations, as no common minimum radiation temperature occurs. Saturation would have the effect of decreasing the difference between the most dense

----

[7]Refer to Spitzer, 1976.

and least dense regions, which, in turn, would decrease the correlations in column density variations.

Values of Tspin were thus seen to vary from less than $\simeq 14+2.7$ K upwards. A simplifying assumption was made in setting the HI spin temperature throughout the cloud to a single value. Observations indicate that the ^{12}CO excitation temperature is $\simeq 10$ K, and this value has been assigned to the HI spin temperature. This temperature choice is likely quite accurate in the coldest regions of most absorption. In warmer regions, this choice had the effect of overestimating column density values, and hence lowering the range of column density values (the dynamic range). The obvious difficulty in estimating Tspin at each of the 1271 points is thus avoided, without incorrectly enhancing the column density variation, and thus the correlation features arising from this data.

In light of the significant uncertainty in this reduction of the data, an effort to test the sensitivity of the autocorrelation techniques to errors in the individual data values was made. This test involved introducing error into the CO column density data through setting each of the column densities to a one bit number[8]. This was done by setting each negative value to -1, and each positive value to +1 after subtraction of the mean. Following this the data

----

[8]One-bit correlation is common of the autocorrelation spectrometers used in radio astronomy, and much has been wirtten about the losses in sensitivity, etc. For a discussion of the signal to noise drop resulting from one-bit analysis ($SNR_{1\ bit} = (2/\pi) * SNR_{analog}$), refer to the early paper by Weinreb, 1963.

had to be reset to zero mean prior to autocorrelation[9]. This one-bit correlation gave remarkably similar results to the true data, with the secondary peaks and overall structure largely unchanged. In light of this, we are confident that significant results were obtainable from our absorption data, even with its unavoidably large errors.

----

[9]See Chapter IV for a discussion of correlation function calculations.

IV. AUTO AND CROSS-CORRELATION ANALYSIS

Correlation analyses[10] are methods generally used to bring to light trends in data which are not apparent from simple observation. They are an attempt to quantify in a statistical sense such trends. In our work the correlations give a measure of mean, large scale structural cloud parameters. The autocorrelation function is a measure of the mean degree of correlation between all pairs of points in a single data set as a function of their spatial separation, vector offset or lag. The cross-correlation function is a measure of the mean degree of correlation between two data sets as a function of lag.

In this work the discrete forms of the two-dimensional auto and cross-correlation functions are employed, where the two dimensional autocorrelation function (ACF) of $F(x,y)$ is given by:

$$FACF(\tau_1,\tau_2) = \frac{(N_1{*}N_2/n_1/n_2){*}\ \Sigma_1\Sigma_2 F(x,y){*}F(x+\tau_1,y+\tau_2)}{\Sigma_1\Sigma_2 F^2(x,y)}$$

and the two dimensional cross correlation function (XCF) of $F(x,y)$ and $G(x,y)$ is given by:

$$XCF(\tau_1,\tau_2) = \frac{(N_1{*}N_2\ /\ n_1/n_2){*}\ \Sigma_1\Sigma_2 F(x,y){*}G(x+\tau_1,y+\tau_2)}{\sqrt{FACF(0,0)}{*}\sqrt{GACF(0,0)}}$$

One can see that as lag increases the number of overlapping points in our discrete ACF (or XCF) drops off linearly, and the first terms above, the ratios of total data pairs to data pairs at the given lag, have been introduced to correct for this. This amounts to introducing a rectangular window

----

[10]See R.N. Bracewell's well-known text for a discussion of correlation techniques and spectral analysis (1978).

23

function in two dimensions, or to "unbiasing" the correlation functions. Unfortunately, another effect of the linear drop off of overlapping data points is that noise becomes gradually more significant as the number of data points decreases and is very high at the edge of the ACF or XCFs (at large positive or negative lags).

It is therefore desirable to apply a two-dimensional window function, as is commonly used in spectral analysis, to the "unbiased" data, having a relatively flat response through the central region, or region of small lags, and dropping off quickly near the edges in the large lag region. For this purpose, the two-dimensional Hamming window function[11] was selected. This function is given for our application as follows:

$$H(\tau_1,\tau_2)=(0.54+0.46*\cos(\pi *\tau_1/\tau_1\max))*$$

$$(0.54+0.46*\cos(\pi *\tau_2/\tau_2\max))$$

This function is similar in effect to the "intermediate" bias employed in the work of Kleiner.

In calculating ACFs, use can be made of the Wiener-Kinchine theorem, which states that the Fourier transform of the autocorrelation function is the power spectrum. Fourier transform methods thus provide us with the capability to indirectly calculate the autocorrelation function through taking the complex transform, calculating from this the power spectrum and then taking the inverse Fourier transform. This method was used[12] and compared with
_____

[11]See Bracewell, 1978 or Stanley, 1975.
[12]Use was made of the efficient Fast Fourier Transform

ACFs calculated directly and no significant difference was observed. Kleiner (1985) suggests that the time savings are enormous through use of FFT routines, but we have found that due to the necessity of doubling and zero padding all arrays as well as fixing array sizes to powers of two, the time savings were not of great import.

As was done by Kleiner, prior to correlation each data set was set to a mean of zero. Smoothing of the correlation images was also done to facilitate easier analysis (contour drawing, etc.). Filtering was performed in the Fourier domain by successive one dimensional transforms in both right ascension and declination followed by multiplication with a "Parzen taper", as discussed by Kleiner, 1985. The side effects of smoothing are the lowering and widening of the large self-correlation spike at zero lag.

Cross-correlations were calculated directly, and divided by the square roots of each of the two self-correlation peak values (zero lag values of the respective ACFs), to facilitate contour level comparison with the two ACF pictures.

It is also of significance that gradients across the field were observed, most notably in velocity. The effect of large gradients is to mask the lower level correlations which are the object of this study. In many cases, it was helpful to have these gradients removed. In order to do

---

[12](cont'd) algorithm in performing the transforms. For a discussion of this algorithm refer to Digital Signal Processing by Stanley, 1975.

this, a best fit plane was subtracted from the data set prior to setting to zero mean and correlation.

Some discussion should now be made of the general appearance of the two dimensional auto and cross-correlation functions. The most striking feature of all autocorrelation functions is the self-correlation peak at zero lag. This peak occurs as a result of the fact that any data set is perfectly correlated with itself. This clearly explains why no central peak is evident on cross-correlation functions. It should also be noted that setting the data to zero mean creates auto and cross-correlation functions with zero mean, making equal regions of positive and negative correlation appear. Finally, all autocorrelation functions are symmetric about the origin, while cross-correlation functions are not.

Autocorrelation of white noise would appear as a delta function surrounded by a zero level. Autocorrelation of a purely repetitive function would appear as a central peak with equally large peaks at single wavelength spacing. Cross-correlation of a repetitive function with a simple disk would give secondary peaks spaced at integer wavelengths.

In many cases the width of the central peak can be a measure of the width of mean structural components of the data. However in much of the following work this information has been lost due to a minimum central width being fixed by the smoothing procedure. This loss of information is unfortunate, but large scale correlations are unaffected,

the study of which is our objective.

V. RESULTS AND DISCUSSION

A. RESULTS

1. MAPS

Figures 3 through 6 are the maps obtained of the region under study. Figure 3 is a contour map of the ^{13}CO (and hence H_2) column density data kindly provided by Kleiner and Dickman. The contour levels in Figure 3 are not actual column densities, as the data provided was scaled arbitrarily. In Figures 4 and 6, the neutral hydrogen column density and velocity maps, the contour levels are physically correct, with the units indicated.

As discussed earlier, there are regions of the map where velocity information could not be obtained. These regions, having zero HI column density, are circled in Figure 5. Inspection of the velocity maps suggests that the method of interpolating velocities was reasonably successful. The regions of no data do not seem to add structure, nor negate structure from the overall velocity map. It was feared that these regions would appear on the interpolated map as hills and valleys, and thus falsely contribute to the velocity autocorrelation function. These regions of zero column density are not clearly outlined on the column density map as a result of smoothing, but it is clear that the two maps are in agreement.

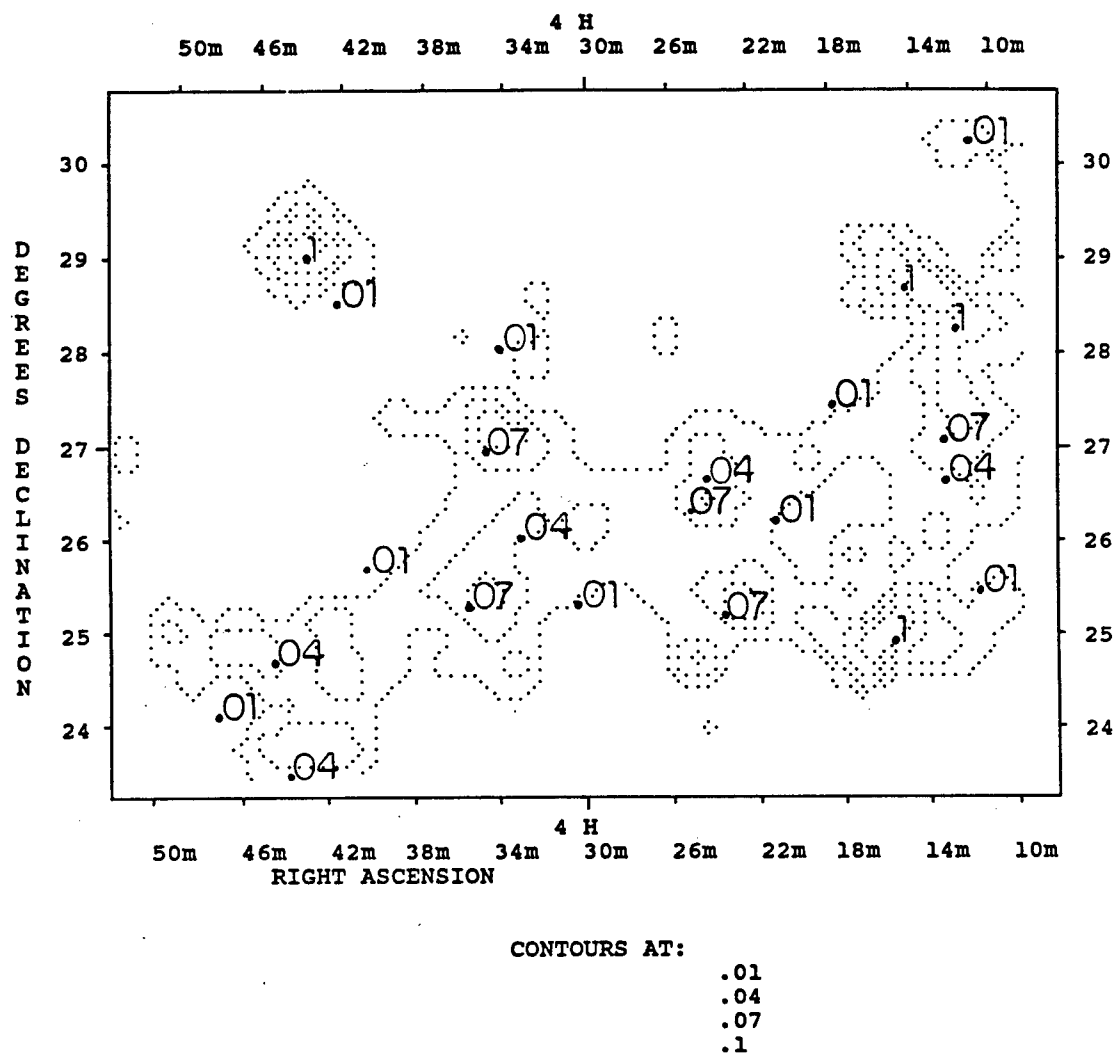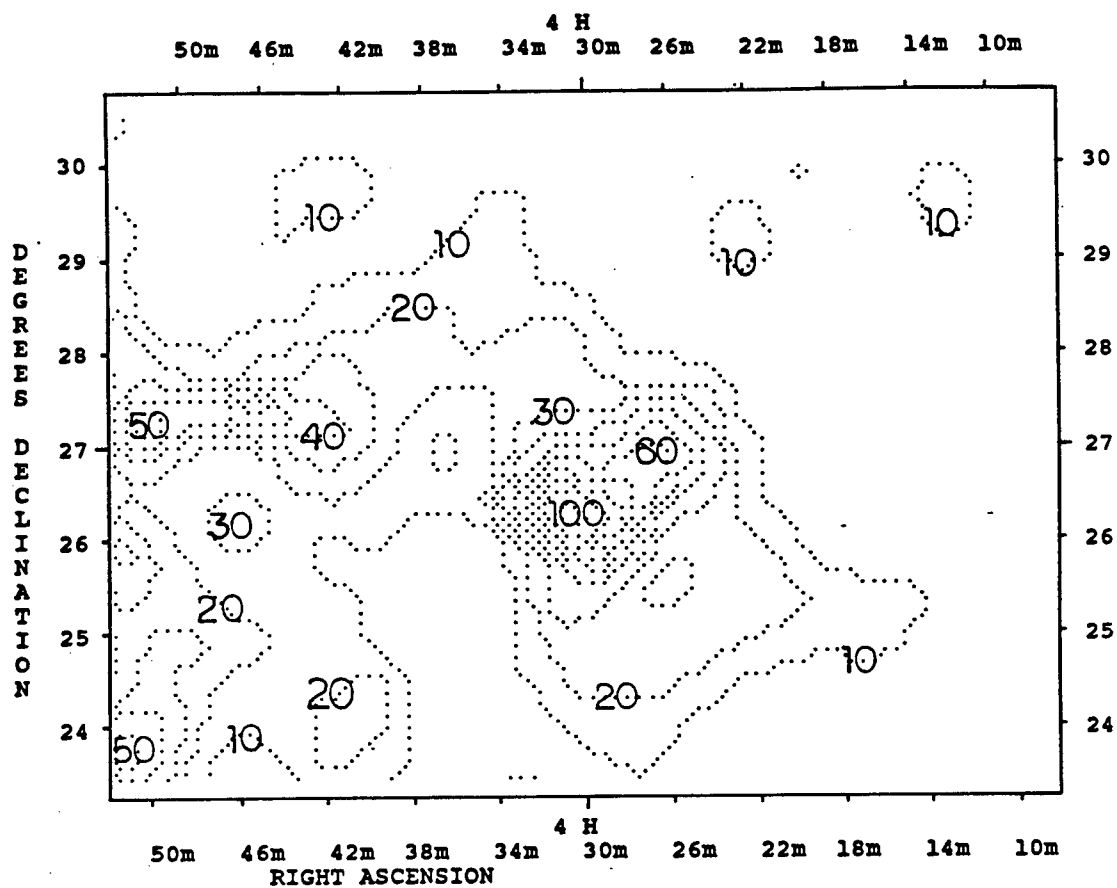Figure 3: Molecular Hydrogen Column Density Map

CONTOURS AT:
.01
.04
.07
.1

Figure 4: Neutral Hydrogen Column Density Map

Figure 5: Regions of Zero Column Density

Figure 6: Neutral Hydrogen Velocity Map

CONTOURS AT:

1 km/sec
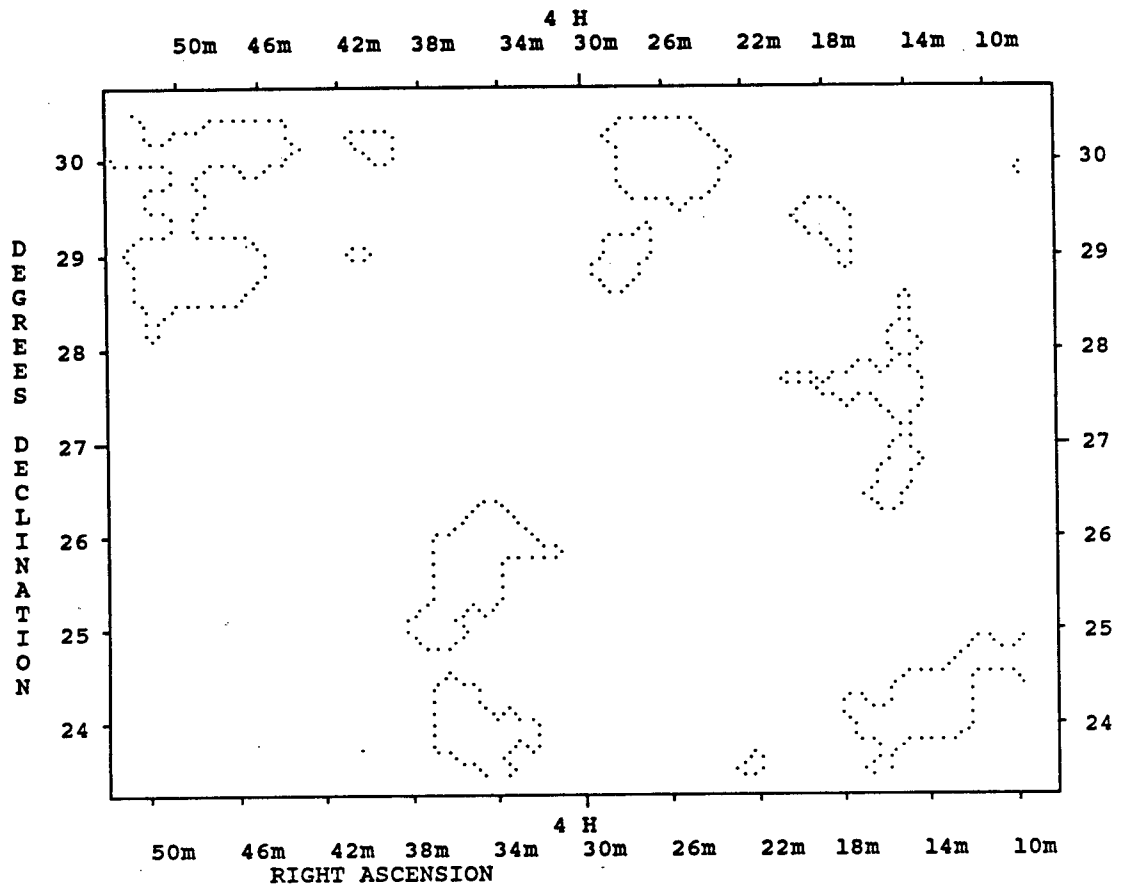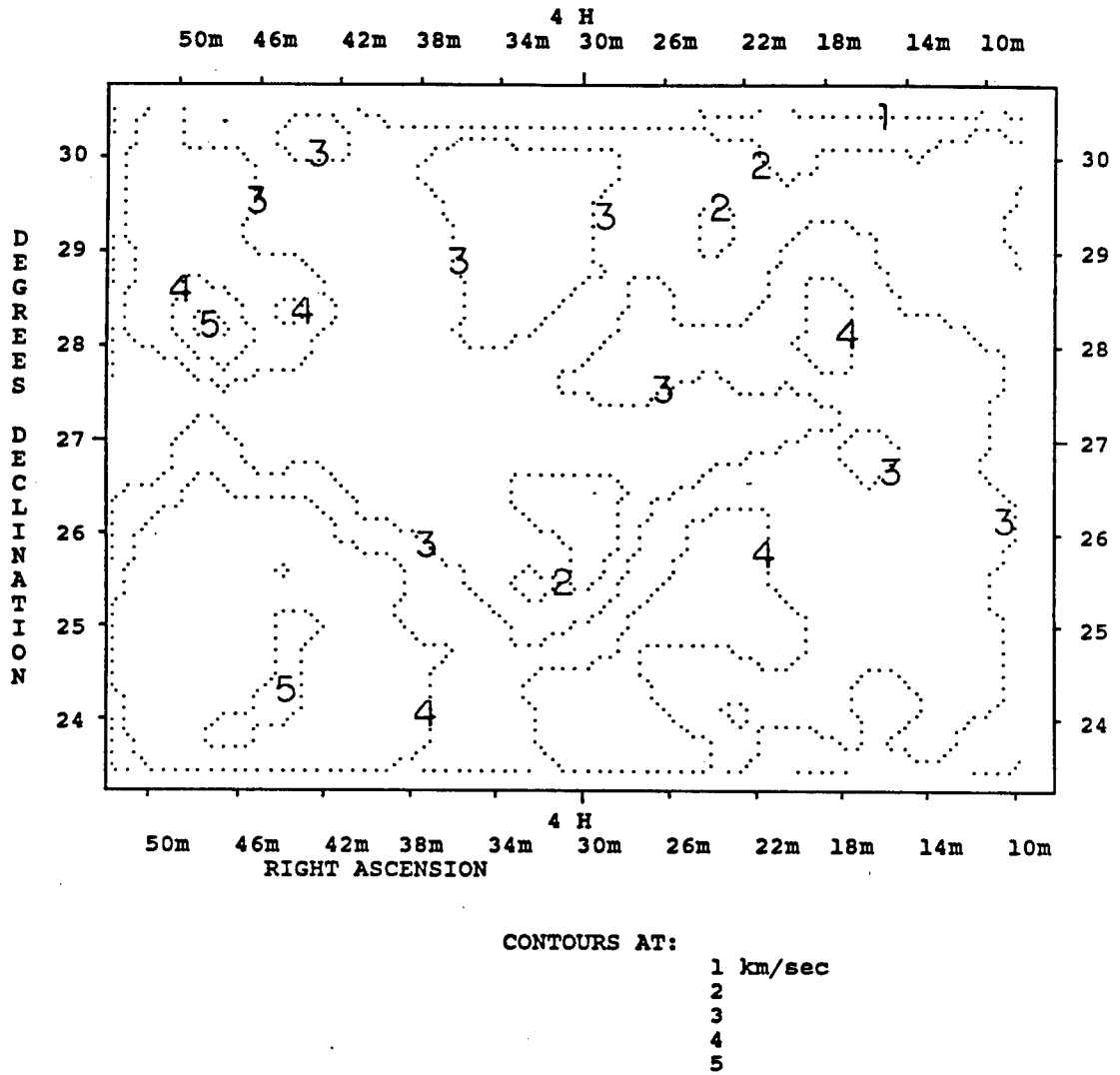2
3
4
5

Comparison of the neutral and molecular hydrogen maps (Figures 3 and 4) shows remarkably different structure in the two components. The H_2 portion of the cloud appears as a roughly elongated structure running from the bottom left to upper right. The HI component is strongly concentrated in the centre of the region with substantial amounts in the left and lower left of the map. Clearly there is also no evidence of a halo of HI gas around the molecular hydrogen.

The neutral hydrogen velocities in the region (Figure 6) are quite discontinuous, demonstrative of there being many components within the region. Superimposed on the motion of the separate pockets of gas is a velocity gradient across the complex evident in the +5 km/sec velocity at the lower left and a +1 km/sec velocity at the upper right. The H_2 velocities also display a gradient of the same magnitude[13], but in the opposite direction.

It was suggested of the H_2 velocity gradient that it was a clear indication of rotation of the elongated complex. The neutral hydrogen, then, appears to be rotating in the opposite direction. Note that neither of the observed rotations is due to Galactic rotation, which will make such objects appear to rotate, but at much slower rates (1/5 of that observed). Furthermore the velocity of the H_2 gas (H_2 velocities ranged from +5 km/sec in the lower left to +9 km/sec in the upper right) appears to be an average of 4 km/sec greater than that of the HI.

[13]No H_2 velocity map is shown as this data was not made available.

2. CORRELATION SURFACES

Autocorrelation functions were calculated for the data shown in the maps of Figures 3,4, and 5. These functions are shown in Figures 7, 8, and 9 on the following pages. Figure 10 shows the cross-correlation of the H_2 and HI column density data.

Figure 7, the H_2 column density autocorrelation function, is essentially identical to that presented by Kleiner, 1985, with slight differences resulting from the smoothing process. A plateau, discussed by Kleiner, extending towards the upper right and lower left is present but very low, with the largest of the secondary peaks located on it near lag (RA,DEC)=(+5.3°,+1.8°) or (-5.3°,-1.8°). Two other slightly lower secondary peaks are also present near lag (+3.8°,-1.7°) or (-3.8°,+1.7°) and near lag (+2°,-4.3°) or (-2°,+4.3°). These secondary peaks are located between 4.2 and 5.7 degrees from the central peak, corresponding to scale lengths between 10 and 14 pc at a distance of 140 pc. The largest of these secondary peaks reaches a level of about 0.055.

Figure 8, the HI column density autocorrelation function, shows an extended twisting plateau, with a secondary peak located near lag (+4.8°,+2.5°) or (-4.8°,-2.5°). This peak appears less significant than that found for H_2, but the level of the plateau is higher, as is the peak (0.065). This peak corresponds to a scale length of about 13 pc.

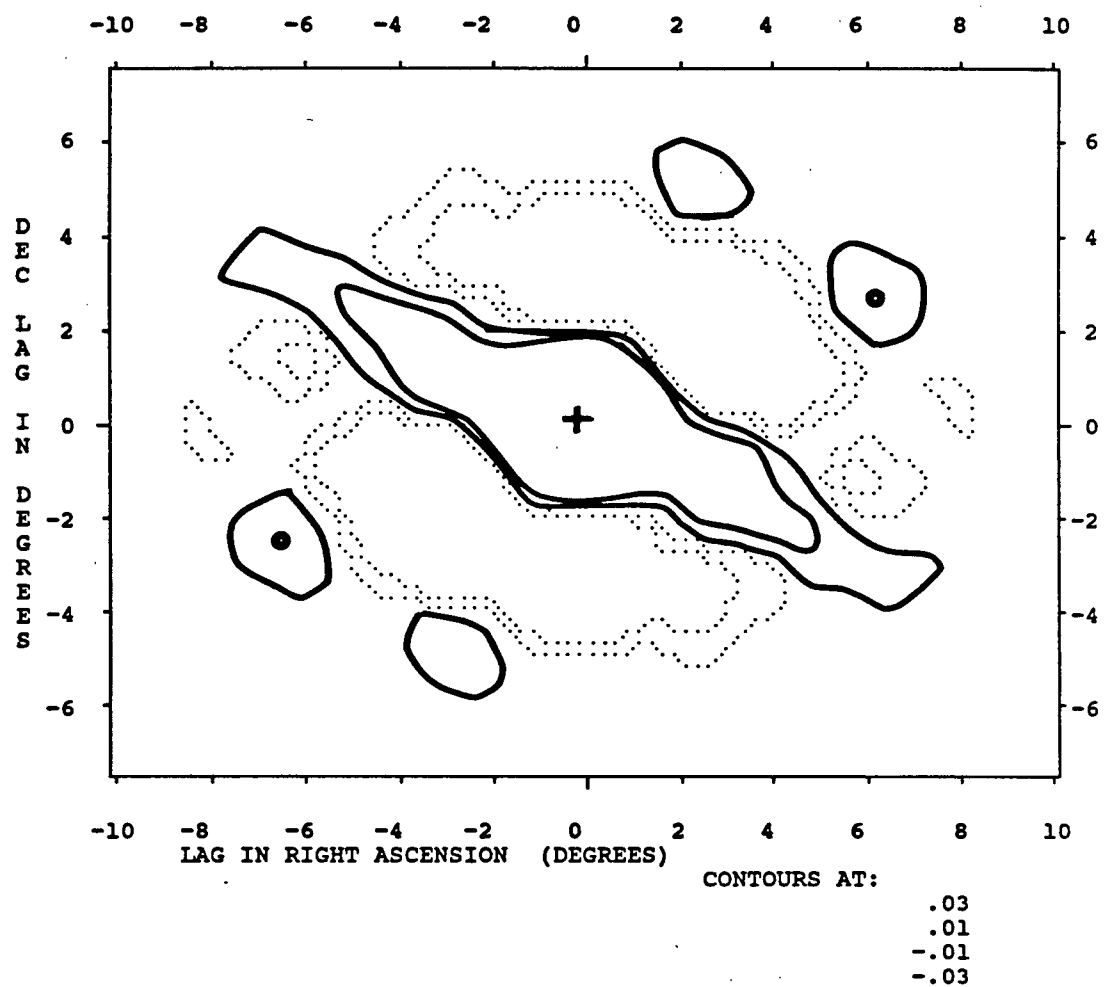Figure 7: Molecular Hydrogen Column Density ACF
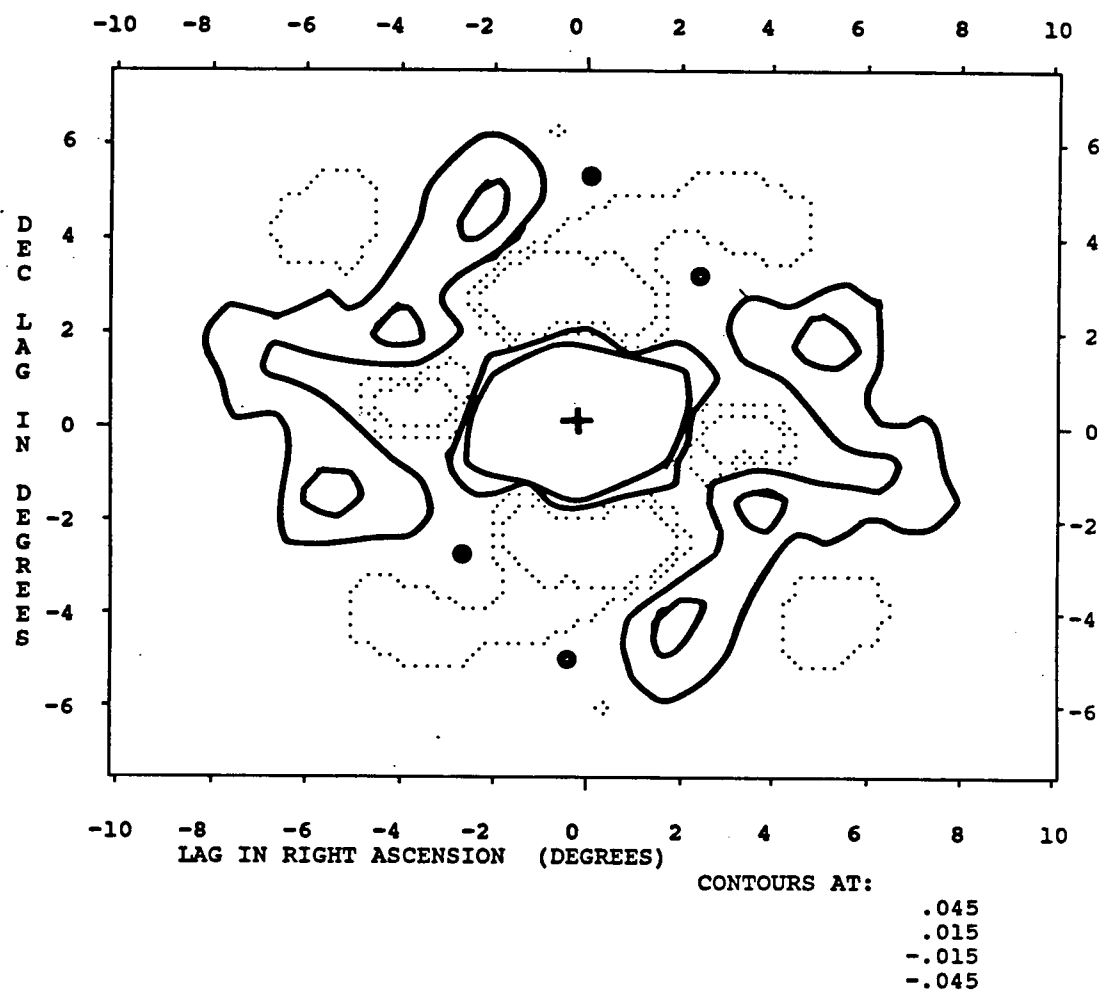
NOTE: Solid Contours Indicate Positive Correlation

Figure 8: Neutral Hydrogen Column Density ACF

CONTOURS AT:

.06
.03
0
-.03
-.06
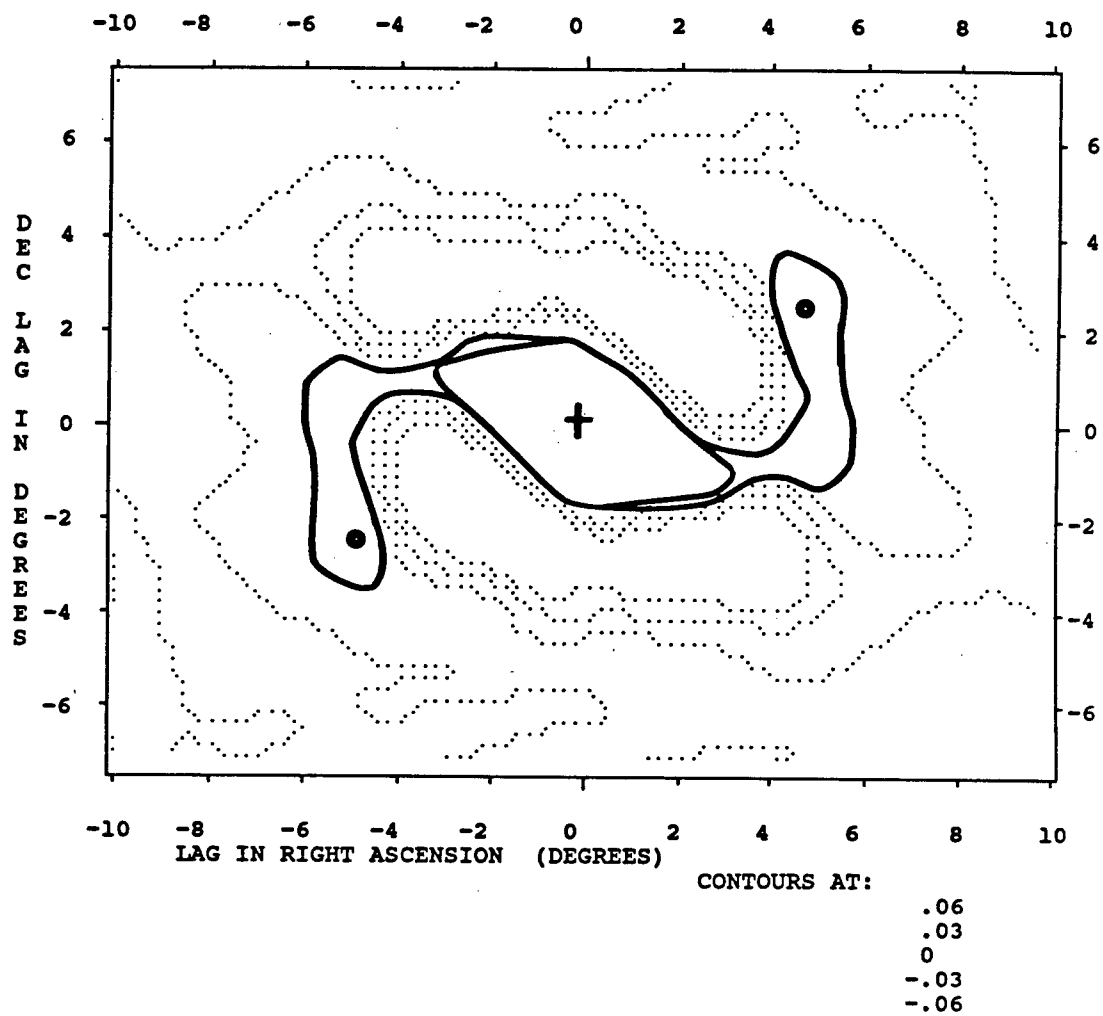
NOTE: Solid Contours Indicate Positive Correlation
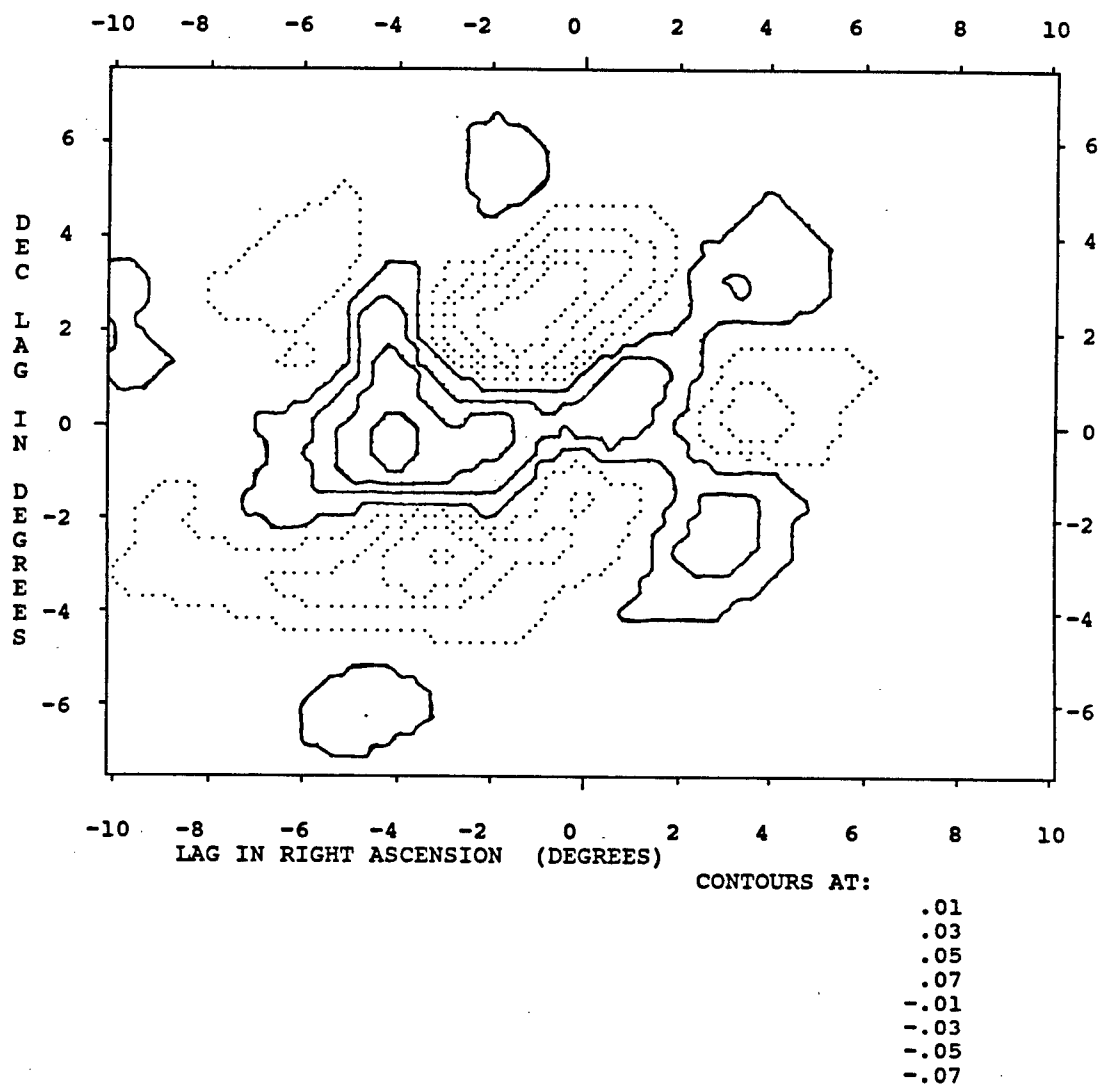
Figure 9: Neutral Hydrogen Velocity ACF

NOTE: Solid Contours Indicate Positive Correlation

Figure 10: XCF of Neutral and Molecular Hydrogen

Column Densities

CONTOURS AT:
.01
.03
.05
.07
-.01
-.03
-.05
-.07

NOTE: Solid Contours Indicate Positive Correlation

Figure 9, the HI velocity autocorrelation function, shows a plateau extending in a different direction having no secondary peak. An isolated secondary peak is, however, evident near lag (+6.1°,+2.7°) or (-6.1°,-2.7°) corresponding to a scale length of 16 pc. The low level of this peak (<0.04) calls its significance into question, especially in light of the large regions of this data which had to be interpolated.

The H_2 and HI column density data were cross-correlated with the results shown in Figure 10. The most interesting feature of this function is the single peak near lag (-4.3°,-0.7°) and the extended plateau to the upper and lower right (note that symmetry no longer holds, nor does a central peak exist). This plateau resembles the main structure of the H_2 map and likely results from the single large peak in the neutral hydrogen map correlating with this structure. All peaks but one are quite low (<0.04) compared to the secondary peaks obtained in either of the column density autocorrelations.

Clearly absent in our statistical analysis is an adequate means of estimating the significance of the correlations observed. One method, which was not implemented due to time constraints (both programming time and running time) is the use of two dimensional Fourier transforms to do Monte Carlo analysis.

In the absence of these, one dimensional power spectra were obtained along selected directions to better illustrate

the correlation lengths quoted. Figures 11, 12, 13 and 14
are normalized power spectra of the H_2 and HI column density
and HI velocity data along axes through the map centre and
in the direction of chief secondary peaks in the respective
autocorrelation function.

Figure 11 shows the power spectrum corresponding to the
largest secondary peak of Figure 7 (near $(5.3°,1.8°)$). The
largest peak in this spectrum represents a scale length of
about 21 pc, likely representative of the plateau structure
which extends in this direction. Figure 12 shows the power
spectrum of an axis through the next highest peak (near
$(3.8°,-1.7°)$). The highest peak corresponds to a scale
length of 12 pc. No plateau is to be seen along this axis.

Figure 13 represents an axis through the secondary peak
located near $(4.8°,2.5°)$ in Figure 8. The peak power is at a
frequency corresponding to a scale length of 14 pc, and this
frequency peak is very dominant.

Figure 14 represents an axis through the secondary peak
located near $(6.1°,2.7°)$ in Figure 9. The peak power is at a
frequency corresponding to a scale length of 16 pc, and
again, this peak is dominant.

B. <u>DISCUSSION</u>

In each of the autocorrelation functions, secondary peaks
were observed at approximately the same orientation, and at
approximately the same distance. Autocorrelation analysis of

Figure 11: Power Spectrum of Molecular Hydrogen Column Density
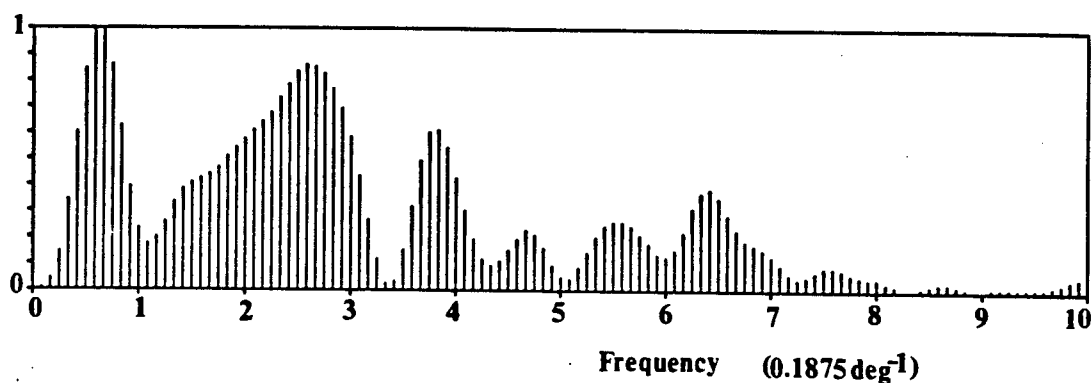
At an angle of +17.5° from constant declination.

Frequency (0.1875 deg⁻¹)

Figure 12: Power Spectrum of Molecular Hydrogen Column Density

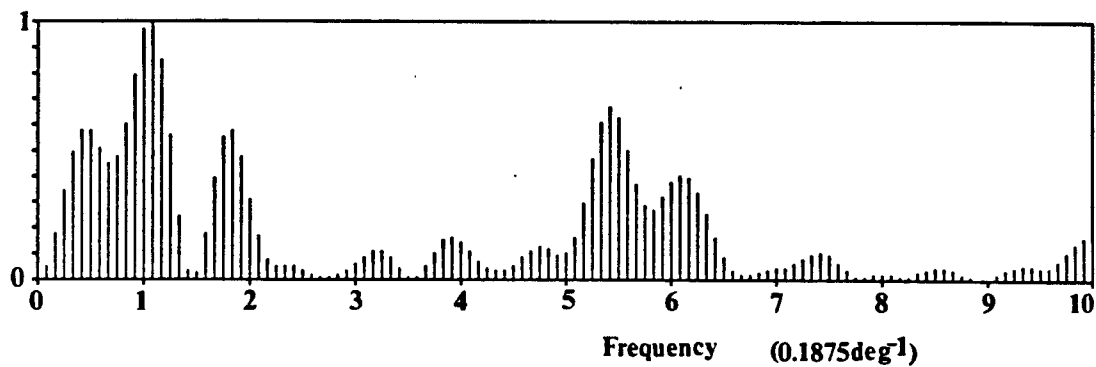At an angle of -25° from constant declination.

Frequency (0.1875 deg⁻¹)

Figure 13: Power Spectrum of Neutral Hydrogen Column Density
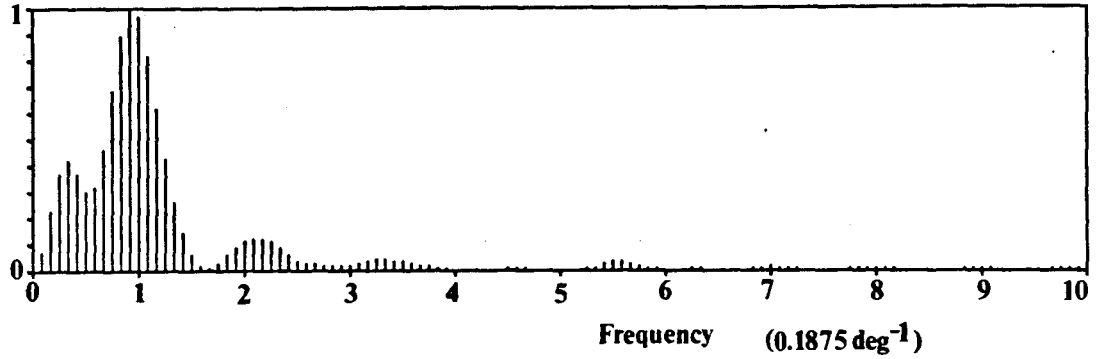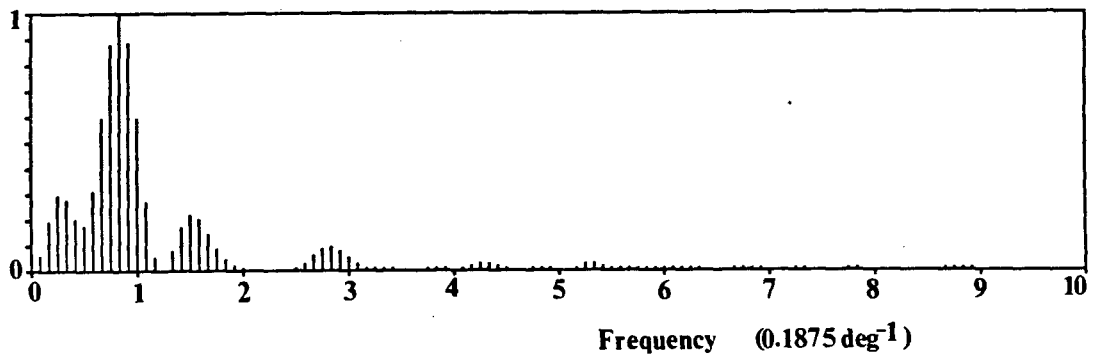
At an angle of +26^0 from constant declination.

Figure 14: Power Spectrum of Neutral Hydrogen Velocity

At an angle of +22^0 from constant declination.

visual extinction in the region from the Lynds catalogue[14] was performed by Kleiner with observed scale lengths of 9 and 14 pc, with the same approximate orientation. The repeated occurance of a $\simeq 14$ pc recorrelation peak in three independent data sets substantially different in appearance strongly suggests a signature of an instability remaining from an early period in the history of the complex when it was more homogeneous.

As discussed above, the Taurus complex is likely extended along an axis 60° to the plane of the sky, and thus a correction for geometrical foreshortening of $(1/\cos\theta)=2$ should be applied. Our observed wavelengths of recorrelation are now 24, 28 and 32 pc.

These scale lengths are clearly not in agreement with the observations of Baker (1973) in which a 7 pc scale length was observed in a one dimensional autocorrelation analysis of warm HI gas. This can be accounted for by the fact that Baker's analysis applied to all of the HI in the line of sight, not an isolated, relatively compact region like the Taurus complex. The 7 pc scale length obtained in Baker's study may well represent some physical phenomena far removed from those being studied in Taurus.

We shall now look at our observed scale lengths in the context of gravitational instabilities in warm HI gas. The Jeans model is a tool used to estimate masses (or densities) at which the onset of gravitational instability occurs. This

----
[14]See Lynds, 1962, the Catalog of Dark Nebulae.

very simple model assumes constant density, zero initial velocity, and zero magnetic field. The hydrodynamic equations simplify to the wave equation[15]:

$$(\nabla^2 - 1/C_s^2 \, \partial^2/\partial t^2 + 4\pi G\rho_0/C_s) \, \rho_1 = 0$$

for which a plane wave density fluctuation is a solution,

$$\rho_1 = A \exp(i(\mathbf{k} \cdot \mathbf{r} - \omega t))$$

satisfying the dispersion relation

$$\omega^2 = k^2 C_s^2 - 4\pi G\rho_0 \, .$$

At $\omega^2 = 0$, a critical value of k is seen at which the disturbance will not grow. This value, k_J, is given by

$$k_J^2 = 4\pi G\rho_0/C_s^2 = 4\pi G\mu\rho_0 m_H / kT \, .$$

For $k < k_J$, ω is imaginary and ρ_1 will grow with time, corresponding to the onset of gravitational collapse. Disturbances for $k > k_J$ are stable oscillations, with the case $k = k_J$ marginally stable.

We will use this simple treatment to estimate an approximate Jeans length in typical HI gas out of which the Taurus complex is believed to have formed. Taking $n_0 = 15$ /cm³, and T=80 K, very reasonable values for a typical warm HI region, a Jeans wavelength (λ_J) of 28 pc is obtained. This value is in general agreement with the autocorrelation scale lengths observed in the Taurus complex.

The Jeans mass is the mass of a spherical region of marginally stable gas, and is given by

$$M_J = (4/3)\pi\lambda_J^3 \rho \, .$$

----

[15]See pages 416, 417 of Astrophysics II by Bowers and Deeming (1984), for a full discussion of this model, or see Mestel, 1965.

For $n_0=15$ /cm^3, this comes out to 3.5 x 10^4 M$_\odot$, consistent with the estimated complex mass of 10^6 M$_\odot$, presumably dispersed amongst a number of unstable regions.

While our observed scale lengths do not appear to be inconsistent with a Jeans-type instability in a warm HI precursor, we are far from demonstrating that this is the case. In fact, the very notion of a long-lived, fossil density structure appears somewhat inconsistent with the notion of Jeans instability, in which such structures are unstable. It is conceivable, however, that unstable condensations would begin at a spacing of about a single Jeans wavelength, and would collapse at this same spacing. A difficulty remains in understanding how the fossil wavelength has remained in the cloud with the seperate clumps moving at different velocities, as shown in Figure 6.

VI. CONCLUSIONS

This work has provided two means of comparison of the neutral and molecular hydrogen constituents of the Taurus molecular complex. Significant differences were found in the HI and H_2 column density maps of the region with neither an HI shell around the H_2 gas nor significant mixing of the two observed. The velocity structures show each gas component to be rotating in opposite directions, with the H_2 velocities an average of 4 km/sec higher than those of the HI.

Average trends in the cloud structure were uncovered by the statistical analysis, primarily an approximately 28 pc recorrelation length observed in each of four data sets analysed. This scale length suggests a large scale instability common to all constituents of the cloud. This scale length approximately corresponds to a Jeans length of instability for warm HI gas, and may correspond to a warm precursor to the present molecular cloud.

The presence of such a scale length in the present cloud is not easily accounted for. The characteristic time for the persistance of correlated structure is likely about the time for a density condensation to travel a single correlation scale length ($\simeq 30$ Myr), and is difficult to reconcile with the notion of a long-lived, "fossil", scale length in the present Taurus complex.

The use of two dimensional correlation techniques was investigated and found to be useful for studies of molecular cloud structure. The single drawback to such analysis is the

absence of a simple, quantitative measure of the
significance of correlation features.

The techniques developed in this work and the previous
work by Kleiner could prove useful in the study of other,
similar, objects. In particular much could be learned if a
second, similar, molecular cloud could be studied.
Unfortunately, the Taurus complex is unique. It remains to
be seen if the scale length observed is a common physical
property of all such clouds or is peculiar to the Taurus
cloud. In addition to this, it may prove feasible to study
the Taurus complex (or other objects) using correlation
techniques on much smaller scales. Such studies are capable
of revealing as much about the small scale structure as this
work did about large scale structure.

BIBLIOGRAPHY

Baker, P.L., *Astronomy and Astrophysics*, <u>50</u>, p. 327, 1976.

Batrla, W., Wilson, T.L. and Rahe, J., *Astronomy and Astrophysics*, <u>96</u>, p. 202, 1981.

Blitz, L., *Scientific American*, <u>246</u>, p. 84, 1982.

Bowers, R. and Deeming, T., *Astrophysics II*, Jones and Bartlett, Boston, 1984.

Bracewell, R.N., *The Fourier Transform and Its Applications*, McGraw-Hill, New York, 1978.

Elias, J.H., *The Astrophysical Journal*, <u>224</u>, P. 857, 1978.

Kleiner, S.C., Ph.D. Thesis, University of Massachusetts, 1985.

Kleiner, S.C., and Dickman, R.L., *The Astrophysical Journal*, <u>286</u>, p. 255, 1984 (Paper I).

Kleiner, S.C., and Dickman, R.L., *The Astrophysical Journal*, <u>295</u>, p. 466, 1985 (Paper II).

Kleiner, S.C., and Dickman, R.L., *The Astrophysical Journal*, <u>295</u>, p. 479, 1985 (Paper III).

Levinson, F.H. and Brown, R.L., *The Astrophysical Journal*, <u>242</u>, p. 416, 1980.

Lynds, B.T., *The Astrophysical Journal Supplement*, <u>7</u>, p. 1, 1962.

Mestel, L., *Quarterly Journal of the Royal Astronomical Society*, <u>6</u>, p. 161, 1965.

Schultz, M.H., *Spline Analysis*, Prentice-Hall, Englewood Cliffs, New Jersey, 1973.

Scoville, N. and Young, J.S., *Scientific American*, <u>250</u>, p. 42, 1984.

Shuter, W.L.H., Dickman, R.L. and Klatt, C., in *IAU Symposium No. 115 on Star Forming Regions*, ed. J. Jugaku and M. Peimbert, In Press.

Spitzer, L., *Physical Processes in the Interstellar Medium*, Wiley, New York, 1978.

Stanley, W.D., *Digital Signal Processing*, Prentice-Hall, Reston, Virginia, 1975.

Weaver, H. and Williams, D.R.W., *Astronomy and Astrophysics Supplement*, <u>8</u>, p. 1, 1973.

Weinreb, S., *MIT Technical Report No. 412*, Dept. of Electronic Engineering, MIT, 1963.